Eur. Phys. J. D **7**, 587–594 (1999)

THE EUROPEAN PHYSICAL JOURNAL D

EDP Sciences

Formation of small water cluster anions by attachment of very slow electrons at high resolution*

J.M. Weber[a], E. Leber, M.-W. Ruf, and H. Hotop[b]

Fachbereich Physik, Universität Kaiserslautern, 67663 Kaiserslautern, Germany

Received 8 March 1999

Abstract. Using a high resolution ($\Delta E \approx 1$ meV) laser photoelectron attachment method, we have studied the formation of $(H_2O)_q^-$ ($q = 2, 6, 7, 11, 15$) cluster ions in collisions of slow free electrons (E = 1–80 meV) and Rydberg electrons (n = 12–300) with water clusters. Resonances at zero energy have been observed, the shapes of which are strongly dependent on cluster size. The results are discussed in terms of the formation of metastable negative ions.

PACS. 34.80.Lx Electron-ion recombination and electron attachment – 36.40.-c Atomic and molecular clusters – 36.40.Qv Stability and fragmentation of clusters

1 Introduction

Due to their importance in many fields of physics and chemistry, the water molecule and its aggregates are of fundamental interest and have been studied for more than 200 years [1]. In the past 20 years water clusters have received increasing attention (for an overview see, *e.g.*, [2,3]). Their properties, such as equilibrium structures of hydrogen bonded networks [4,5], or the change of electronic structure from the single molecule to bulk [2,3,6], have been studied not only for neutral, but also for charged clusters.

Anion formation in the interaction of low energy electrons with molecular clusters often proceeds through resonances known from the molecular constituent, but additional features are observed which reflect the effects of the cluster environment on the resonance energy and symmetry [7–9]. One fascinating result in such studies of cluster anion formation is the observation of a strong resonance at zero energy (the indicator of an s-wave attachment process) in cases where such a feature is absent in the monomer (see, *e.g.* [7,8,10–14]). Negative ion formation in the collision of a cluster $(XY)_N$ (described by a set of quantum numbers $\{\alpha\}$ denoting its electronic and ro-vibrational state) with an electron may proceed along several reaction pathways through a temporary negative ion $(XY)_N^{-*}$:

$$(XY)_N\{\alpha\} + e^-(E) \rightarrow (XY)_N^{-*}$$
$$\rightarrow (XY)_N\{\alpha'\} + e^-(E') \quad (1a)$$
$$\rightarrow (XY)_q Y^- + X + (N-q-1)XY \quad (1b)$$
$$\rightarrow (XY)_q^- + (N-q)XY \quad (1c)$$
$$\rightarrow (XY)_N^{-\ddagger} \quad (\tau > 100\ \mu s) \quad (1d)$$
$$(+M) \rightarrow (XY)_N^- \quad (1e)$$
$$\rightarrow (XY)_N^- + \gamma. \quad (1f)$$

In resonant elastic ($\alpha = \alpha'$) or inelastic scattering processes (1a) the electron is re-emitted from the cluster, *i.e.* no long lived negative ion is formed. If energetically possible, dissociative attachment processes (1b) may occur, resulting in a negative ion $(XY)_q Y^-$ and neutral fragments (as is the case for, *e.g.*, N_2O clusters [7,12,14]). If the adiabatic electron affinity (AEA) of a cluster of size p ($q \leq p \leq N$) is larger than the binding energy of a monomer XY to this cluster, the temporary negative cluster ion $(XY)_p^-$ may evaporate monomers until a stable anion is formed. This evaporative attachment process (1c) is found in many cluster systems [7,8,15], for example for $(O_2)_N$ [10,13,16]. Even if no other stabilizing process occurs, the temporary negative ion $(XY)_N^{-*}$ can become metastable with respect to spontaneous re-emission (autodetachment) of the electron, if the electronic energy is rapidly redistributed into internal degrees of freedom (intra- and intermolecular vibration, rotation), thereby yielding the long-lived negative ion $(XY)_N^{-\ddagger}$ (1d). Finally, the negative ion can be stabilized by a collision with a third particle M (1e). Radiative attachment (1f)

* Work based on Chapter 9 of the unpublished doctoral dissertation of Jörg Mathias Weber (Fachbereich Physik, Universität Kaiserslautern, December 1998).

[a] *Present address*: Department of Chemistry, Yale University, P.O. Box 208107, New Haven, CT 06520-8107, USA.

[b] e-mail: `hotop@physik.uni-kl.de`

is normally a negligible path; typical cross-sections are estimated to be $\leq 10^{-26}$ m^2 for electron energies > 1 meV, using detailed balance with an electron affinity of about 0.03 eV (as relevant for the water dimer [17]) and a photodetachment cross-section of $\leq 10^{-20}$ m^2 (see [18]).

Similar reactions take place through the transfer of an electron from a highly excited Rydberg atom. If the principal quantum number n of the Rydberg atom is high enough that one may neglect post-attachment effects associated with the Coulomb attraction of the formed ion pair (for n larger than about 40) one can assume that the Rydberg electron behaves essentially like a free electron [19–22]. One can thus use Rydberg electron transfer (RET) to probe electron attachment behaviour at very small electron energies (see, *e.g.*, [22]). The rate coefficient $k_{n\ell}$ for RET is then given by [21,22]

$$k_{n\ell} = \int_0^\infty \sigma_{\mathrm{e}}(\upsilon)\upsilon f_{n\ell}(\upsilon)\,\mathrm{d}\upsilon, \qquad (2)$$

$\sigma_{\mathrm{e}}(\upsilon)$ denoting the velocity dependent attachment cross-section for free electrons, and $f_{n\ell}(\upsilon)$ the velocity distribution function of a Rydberg electron with principal quantum number n and angular momentum ℓ [21]. For an s-wave attachment process, $\sigma_{\mathrm{e}}(\upsilon)$ behaves like υ^{-1} in the limit of $\upsilon \to 0$, one therefore would observe RET rate coefficients that are independent of n and ℓ; an example that comes close to this behaviour is RET to SF_6 molecules (see, *e.g.* [22]). At lower principal quantum numbers the RET rate coefficients may behave differently due to two effects: peaks in the n dependence associated with the formation of weakly bound negative ions through curve crossing processes [23,24], and post-attachment effects towards lower n ($n < 40$) associated with the Coulomb interaction of the ionic Rydberg core and the newly formed negative ion [22].

Single water molecules cannot bind additional electrons, and free H_2O^- ions have never been observed. However – similar to the case of ammonia and its aggregates – the electron affinity is positive in the condensed phase, giving rise to solvated (or in this special case hydrated) electron states (see, *e.g.* [3]). Some of the important aspects and questions in connection with water cluster anions $(H_2O)_q^-$ are:

- How many water molecules must be present in a cluster to bind an extra electron?
- What are the binding energies of the states of excess electrons as a function of cluster size, and how strongly localized is the extra electron?
- How do neutral and anionic clusters of the same size differ in their respective equilibrium structures?
- How does the state of the excess electron evolve from the minimum cluster size to the condensed phase?
- What happens in the process of electron attachment to water clusters?

Theoretical studies on excess electron states in water clusters have been performed by several authors [17,25–32]. Detailed studies by Barnett *et al.* [25] predicted for small anions ($q = 2, 8$) a delocalized electron in a spatially large orbital (typical radii ranging from $9.3a_0$ for $q = 8$ to more than $36a_0$ for $q = 2$), weakly bound by the total dipole moment of the cluster (the molecular electric dipole moment is 1.854 Debye [33], that of the dimer amounts to 2.643 Debye [17]). For larger clusters they expected the excess electron state to evolve from a state solvated at the surface of the cluster to internally bound states, completely surrounded by a network of water molecules. Calculations by Kim and coworkers [28–30] predict an internally bound state already for $q = 6$, Tsurusawa and Iwata [32] even believe internal states in the dimer and trimer anions to be possible. However, no experimental evidence has been found for internal states in water cluster anions this small.

Early experiments on the attachment of slow electrons to water clusters by Haberland *et al.* [34] showed that dimer anions $(H_2O)_2^-$ are formed by injection of slow electrons into the condensation zone of a supersonic beam of water vapor seeded in Ar. Knapp *et al.* [11] found substantial signals due to long lived cluster anions with $q \geq 11$ in collisions of slow electrons from a hot filament (energy resolution $\Delta E \approx 1$ eV) with preexisting water clusters under single collision conditions (*i.e.*, after condensation), indicative of an s-wave process. Schermann and coworkers [17,33,35–37] studied in detail Rydberg electron transfer (RET) reactions to water clusters and water-containing heterogeneous clusters. They attributed their findings for small clusters ($q = 2, 6, 7$) to the formation of dipole-bound anions with small binding energies, in accord with theoretical predictions by Barnett *et al.* [25].

The electronic properties of water cluster anions have been studied by several authors using photodestruction of the negative ions [18,38–43]. The behavior of the vertical detachment energy (VDE) as a function of cluster size observed in photoelectron spectroscopy experiments by Coe *et al.* [39] has been interpreted to be consistent with the existence of internal states for cluster ions with $q \geq 6$, as they fit to a curve predicted by Barnett *et al.* [25] for a spherical charge distribution in a uniform dielectric. Additional peaks with higher VDE's for $q = 2, 6, 7$ have been attributed to dipole bound or surface states. Johnson and coworkers reported similar photoelectron spectra, but discussed their results in terms of surface bound states for the peaks associated with higher electron binding energies, while they assigned the more weakly bound states observed in the photoelectron spectra for small cluster ions ($q = 2, 3, 5$–$8, 10, 11$) to be dipole bound [18,43]. By comparison of the results for hydrated electrons with results of hydrated I^- ions (residing on the surface of the host cluster) they showed the "polarized dielectric" model to be ambiguous with respect to judging the binding site of the excess electron [18]. The evolution from the surface-bound to the internal state [6], as predicted by Barnett *et al.* [25], has never been found to be mirrored in photoelectron spectra. Johnson and coworkers also studied the branching ratio of the decay of photoexcited $(H_2O)_m^{-*}$ ions (photoabsorption cross-sections up to several 10^{-20} m^2 [18] at photon energies around 0.8–1.2 eV) into photofragmentation

and photodetachment channels as a function of photon energy [38]. They found strong competition between these two channels near the photodetachment threshold, while photodetachment is the dominant decay channel at higher photon energies. For the decay of temporary negative ions formed in electron attachment to water clusters, they predicted in analogy to their photodestruction results that autodetachment should be the dominant decay channel, especially at higher electron energies. Experiments dealing with the associative detachment reaction of D_2O molecules with water cluster anions as a function of cluster size [44], and thermal destruction of negative ions of water clusters in H_2 buffer gas [45] suggest that the binding energy of a water molecule to a water cluster anion is larger than the adiabatic electron affinity of the cluster for clusters with less than about 15 water molecules.

In this work we present experimental results on the formation of small negatively charged water clusters $(H_2O)_q^-$ in electron attachment to preexisting water clusters in the energy range 1–80 meV at an electron energy resolution of ≤ 1.5 meV, using a laser photoelectron source. We report the observation of size dependent resonances at zero energy in the formation of cluster anions by electron attachment, for the first time also for ions with less than 11 molecular constituents. Our results are discussed in terms of coupling of the electronic and intermolecular vibrational degrees of freedom, yielding metastable negative ions. We have also performed electron transfer measurements from $K^{**}(ns, nd)$ Rydberg atoms to water clusters, extending the range of previous work by Schermann and coworkers [17,35] up to principal quantum numbers $n \approx 300$. By comparison of calculated rate coefficients [21], derived from the shape of the zero energy resonances in free electron attachment with the measured RET rate coefficients we examine the validity of the free electron model for Rydberg electrons [19–22].

2 Experimental

Our experiment is based on the Laser Photoelectron Attachment (LPA) method introduced by Klar *et al.* [46,47]: energy-variable, monoenergetic electrons are created by photoionization of atoms in a collimated beam; they interact with the target molecules (clusters) of interest in the region where the photoionization process takes place. The first LPA experiments involved a static molecular gas target of several polyatomic molecules including SF_6 [46] and CCl_4 [48]. Recently, the LPA method has also been used in combination with a skimmed supersonic beam, and unprecedented resolution down to 20 μeV has been achieved [49]. While in our previous LPA investigations photoionization of laser-excited $Ar^*(4p, J = 3)$ atoms yielded electron currents up to 1 pA, we have now used an analogous scheme with a demonstrated potential for nA currents, namely photoionization of laser-excited $K^*(4p_{3/2})$ atoms. A schematic view of the present LPA apparatus is shown in Figure 1. Both hyperfine components of ground state $^{39}K(4s, F = 1, 2)$ atoms in a collimated

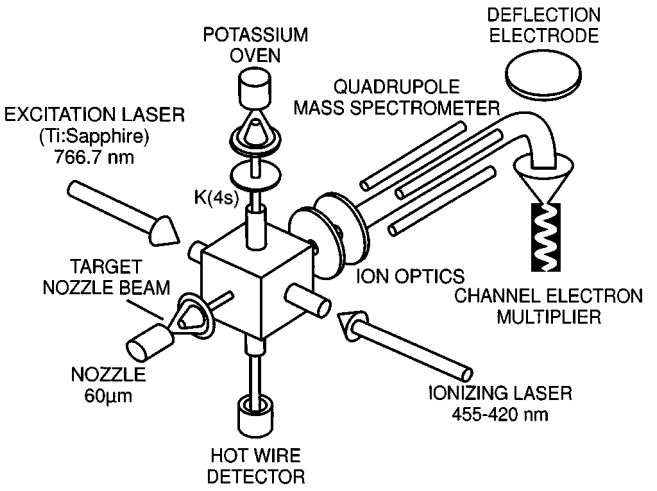

Fig. 1. Schematic view of the present LPA apparatus (see text).

beam of potassium atoms (collimation 1:400, diameter 1.5 mm) from a doubly differentially pumped metal vapor oven are simultaneously excited to the $^{39}K^*(4p_{3/2}, F = 2, 3)$ states by a transverse CW two frequency Ti:sapphire laser ($\lambda = 766.7$ nm). Part of the excited state population is transferred to high Rydberg levels $(nd, (n+2)s, n \geq 12)$ or photoionized by interaction with the intracavity field of a broadband (40 GHz) tunable dye laser (power up to 5 W), operated in the blue spectral region ($\lambda = 472$–424 nm, dye Stilbene 3). The energy of the photoelectrons can be continuously varied over the range 0–200 meV by tuning the wavelength of the ionizing laser ($\lambda < 455$ nm).

Free or Rydberg electrons, created in the overlap volume of the K atom and the laser beams, may attach to molecules and clusters in a collimated, differentially pumped nozzle beam (diameter in the reaction region 3 mm; nozzle diameter $d_0 = 60$ μm, stagnation pressure $p_0 = 4.9$ bar, nozzle temperature $T_0 = 40$ °C), propagating in a direction perpendicular to both the potassium and the laser beams. For the sake of normalization and resolution testing, using the well-known cross-section for SF_6^- formation from free electron attachment to SF_6, the target gas mixture contains 0.15–0.3% of SF_6 molecules. The gas mixture in the present experiment is prepared by flowing carrier gas (containing trace amounts of SF_6 as mentioned above) over a water surface in a stainless steel container, which is kept at $T = 25$ °C, thereby saturating the carrier gas with water vapor (partial pressure about 32 mbar). As several authors have mentioned before (see, *e.g.*, [34,35,42,43]), the intensities of $(H_2O)_q^-$ ion signals depend on the cluster source conditions. We have used He as a carrier gas studying the formation of the dimer negative ion, and Ne for all other cluster sizes under study.

The reaction volume is surrounded by a cubic chamber made of oxygen free, high conductivity copper, the inner walls of which are coated with colloidal graphite. By applying bias potentials to each face of the cube, DC stray electric fields are reduced to values $F_S \leq 70$ mV/m. Magnetic fields are reduced to values below 2 μT by compensation coils located outside the vacuum apparatus.

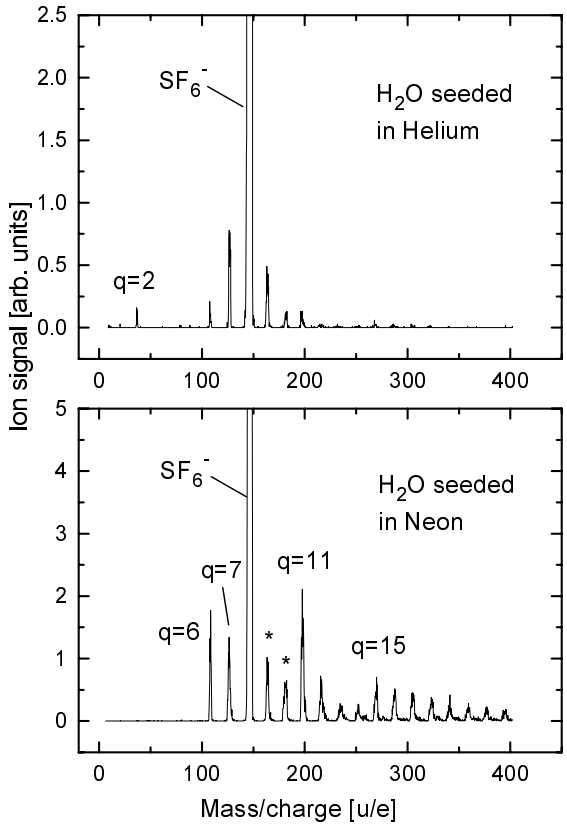

Fig. 2. Rydberg electron transfer (RET) mass spectra (principal quantum number $n \approx 300$) taken with He (upper trace) and Ne (lower trace) as carrier gases. Peaks marked with asterisks are due to heterogeneous cluster ions $(H_2O)_m \cdot SF_6^-$ (see text). The nozzle beam (nozzle diameter 60 μm) was operated at a stagnation pressure of 4.9 bar and a nozzle temperature of 40 °C.

The electron energy resolution is limited by the bandwidth of the ionizing laser ($\Delta E_L \approx 150$ μeV), residual electric fields ($\Delta E_F \leq 245$ μeV), the Doppler effect caused by the target velocity ($\Delta E_D \approx 0.07\sqrt{E}$, ΔE_D and electron energy E in meV), and space charge effects due to K^+ photoions generated in the reaction volume (depending on the K^+ current). An upper limit to the overall energy spread close to $E = 0$ eV can be estimated by comparison of the SF_6^- ion yield, measured under the same conditions as the cluster ion yield, with the cross-section measured by Klar *et al.* [46] at sub-meV resolution. For the present experiment electron currents around 22 pA were chosen, resulting in an overall resolution of $\Delta E_{max} \approx 1.2$ meV.

Anions, generated by electron attachment and drifting out of the essentially field free reaction chamber, are imaged into a quadrupole mass spectrometer ($m/q \leq 2000$ u/e) and detected by a differentially pumped off axis channel electron multiplier. Cluster ions of the sizes $q = 2, 6, 7, 11, 15$ have been chosen for closer inspection due to the pronounced ion signal intensities (see Fig. 2). Relative ion formation cross-sections for free electrons have been measured by keeping the mass spectrometer tuned to a particular mass while varying the electron energy. In contrast, RET rate coefficients have been derived by keeping the blue laser tuned to a specific photon energy while taking mass spectra. Here, the SF_6^- signal has been used for calibration.

In electron attachment to SF_6 molecules, small amounts of SF_5^- ions are formed (typically 10^{-3} of the SF_6^- ion count rate at the same electron energy). As the resolution of the mass spectrometer ($m/\Delta m \approx 53$ FWHM) is insufficient to properly distinguish between the peaks of SF_5^- ($m = 127$ u) and of the water heptamer ion $(H_2O)_7^-$ ($m = 126$ u), the heptamer ion signals were corrected by subtracting 10^{-3} of the SF_6^- ion count rate from the raw "heptamer" ion count rate, amounting to about 10% of the uncorrected count rate. Heterogeneous cluster ions $(H_2O)_m \cdot SF_6^-$ are 2 u heavier than ions of the stoichiometry $(H_2O)_{m+8}^-$, a mass difference that is not completely resolved either, but signals in the wings of the mass peaks due to heterogeneous species are negligible compared to the respective peak signals of the homogeneous cluster ion signals, their contribution has thus been ignored for measurements involving free electrons. For deriving RET rate coefficients, the mass peaks of $(H_2O)_{11}^-$ and $SF_6^- \cdot (H_2O)_3$ have been distinguished by fitting two Gaussians with the respective center positions and widths to the combined peak in the respective mass spectra. Test measurements without SF_6 assured that the water cluster ion signals (apart from $q = 7$, see above) do not depend on the presence or absence of SF_6 in the target gas mixture.

3 Results and discussion

Figure 3 shows the relative rate coefficients $k_e(E) = \sigma_e(E)v_e \propto \sigma_e(E)E^{1/2}$ (σ_e: relative ion formation cross-section, v_e: electron velocity) for the formation of $(H_2O)_q^-$ ions ($q = 2, 6, 7, 11, 15$) as a function of electron energy ($E = 1$–80 meV). The rate coefficients have been normalized such that the respective relative ion yields amount to 1000 for RET at very high principal quantum numbers ($n \approx 300$). One observes a very steep drop of the rate coefficient for the formation of the dimer ion at very low electron energies. Note that for s-wave attachment to molecules without electric dipole moment one expects an energy independent rate coefficient for sufficiently low electron energies [22,46,47]. The rate coefficients for $q = 6, 7$ decrease less strongly than for $q = 2$; in addition, one observes significant signals at higher electron energies ($E \geq 30$ meV) for $q = 7$, giving rise to a broad feature that dominates the energy dependence for $q = 11, 15$. The fact that no "zero eV resonances" for $q \leq 10$ have been reported yet, may be due to the much broader electron energy distributions in previous work, preventing the observation of resonances this sharp.

If one wants to understand the process of the formation of negatively charged water cluster ions $(H_2O)_q^-$ from a neutral cluster $(H_2O)_N$ ($q \leq N$), one has to analyze the possible reaction pathways of the temporary negative ion (see Eqs. (1a–1e)). Channels (1a) and (1b) do not yield homogeneous $(H_2O)_q^-$ ions. The channel of stabilization

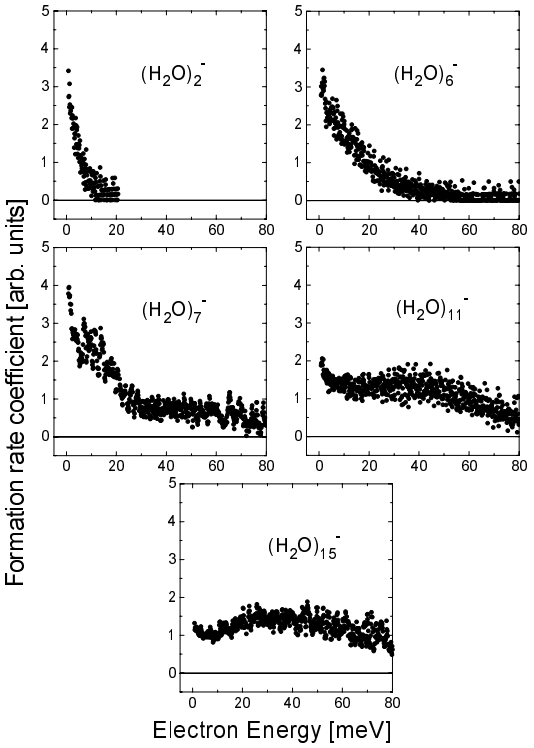

Fig. 3. Relative rate coefficients for formation of $(H_2O)_q^-$ ions in the energy range $E = 1$–80 meV. The values have been normalized such that the corresponding ion yields amount to 1000 for RET at very high principal quantum numbers ($n \approx 300$). For $q = 7, 15$ the values have been averaged over 5 channels, respectively. Ion count rates were very small, especially for the dimer (1–2 s^{-1} at $E = 5$ meV, 30 s total integration time per channel for the dimer). The scatter of the data points represents the statistical $\sqrt{N}$ error.

by collision with a third particle (1e), however, has to be analyzed more closely. In RET from Rydberg atoms with quantum numbers $n \leq 40$ the core of the Rydberg atom could serve as a collision partner for reaction (1e). However, for RET at very high principal quantum numbers and for free electrons the only particles to stabilize a temporary negative ion through a collision would be K^+ ions, generated along with the free electrons in the photoionization process. The autodetachment lifetime of the anions primarily formed by electron attachment would have to be large compared to the transit time of the ions through the space charge region to allow a substantial stabilization efficiency. In order to estimate the cross-sections $\sigma_{\rm stab}$ necessary to stabilize only 1% of the temporary negative ions by this process, one has to evaluate the term

$$I_{\rm stab}/I_0 = 1 - \exp(-\sigma_{\rm stab} n_+ d) \approx 0.01, \qquad (3)$$

where $I_{\rm stab}$ is the number of stabilized ions, I_0 the number of ions primarily generated by electron attachment, n_+ the ion density (about 120 mm^{-3} for the present experiment), and d the mean distance that a negative ion travels through the space charge region (about 1 mm). With the present experimental conditions one derives a necessary stabilization cross-section of 8.2×10^{-11} m^2, which we judge to be too high to be likely. Moreover, estimating the minimum transit time for a water cluster ion through the thin K^+ cloud to be about 0.5 μs (using the velocity of the He carrier gas of 1800 m/s), the lifetime of the temporary negative ion with respect to re-emission of the extra electron would have to be on the order of μs, which is unlikely without redistribution of the electronic energy into internal degrees of freedom of the cluster. This redistribution process, on the other hand, allows access to the channels of evaporative attachment (1c) and formation of metastable ions (1d).

Table 1. Energetics relevant for electron attachment to water clusters.

Cluster size q	$E_{\rm B}(q)$ [meV][a]	$AEA(q)$ [meV][b]	$VDE(q)$ [meV][c]
2	450	30 ± 4	50
6	475	111	480
7	642	121	490
11	637	146	720
15	547	414	–

[a] Binding energies of a water molecule to a neutral cluster consisting of q water molecules. The values are taken from Table 1 in [5].
[b] Adiabatic electron affinities; the dimer value is taken from [17], all other values are estimates of the AEA by linear interpolation, using the quoted dimer value and the values for $q = 8, 12, 18$ for surface bound states from [25]; estimated errors amount to ± 100 meV, if not otherwise stated.
[c] Vertical detachment energies taken from Table 1 in [43], the errors are given as ± 30 meV in the quoted paper.

Evaporative attachment is only possible, if the binding energy $E_{\rm B}$ of a water molecule to a neutral cluster of size q is smaller than the adiabatic electron affinity (AEA) of that cluster, which has been found to be the case only for clusters with more than about 15 molecules [44,45]. Unfortunately, the AEA of most water clusters have not yet been determined with great accuracy. In order to roughly estimate those values, one can use a linear interpolation, taking the AEA of the dimer known from RET experiments [17] and the values calculated by Barnett *et al.* [25] for surface bound states of $q = 8, 12, 18$. The vertical detachment energies measured by Johnson and coworkers [43] and attributed to surface bound states may serve as upper limits. For the binding energies of additional water molecules we use the values given in [3]. The relevant data are summarized in Table 1. The interpolated AEA values are significantly smaller than the respective $E_{\rm B}$ for all cluster sizes under study, and the assumed upper limits are only on the order of their respective $E_{\rm B}$ values. Although the water clusters will have a finite temperature before the attachment process, the energy amount in each vibrational coordinate will not be enough to promote evaporation. Only for $q = 15$, the combined AEA and internal energy may be sufficient to allow thermal emission of one cluster constituent upon electron attachment to a neutral cluster of $q + 1 = 16$ water molecules. If the parallel between a photoexcited negative cluster ion

Table 2. Analytical parameterization of the free electron cross-sections for ion formation: two parameters denoted p_1 and p_2 were used. The functions represent the cluster ion yields in the energy range 1–20 meV, we assume that the analytical behaviour can be continued also for electron energies below 1 meV. Parameterization functions were (E in meV).

Cluster ion size q	Function	p_1	p_2
2	exponential[a]	0.03049	3.120
6	modified Klots formula[b]	0.0511	1.23
7	modified Klots formula[b]	0.0730	0.670
11	modified Klots formula[b]	0.106	0.171
15	modified Klots formula[b]	0.759	0.015

[a] An exponential function $\sigma(E) = p_1 \exp(-p_2 E)$ for dimer formation.

[b] A modified Klots-type formula [21,46,47,52] $\sigma(E) = p_1 E^{-1}[1 - \exp(-p_2 E^{1/2})]$; this expression behaves as Wigner's threshold law for s-wave attachment ($\sigma \propto E^{-1/2}$) in the limit for $E \to 0$, and as E^{-1} (s-wave scattering cross-section) for large energies.

and a temporary negative ion formed in electron attachment drawn by Johnson and coworkers [38] holds, autodetachment of the extra electron should be the dominant process, even if evaporation is energetically allowed.

The only process left to explain the observation of water cluster anions at low electron energies is the formation of metastable ions, *i.e.*, we assume that the electronic energy is rapidly redistributed among the internal degrees of freedom of the cluster, most probably in "soft", intermolecular vibrational modes [17,50]. This conclusion is consistent with the observation that the relative rate coefficient for dimer anion formation decreases much more rapidly than that for hexamer anion formation, as the hexamer has more intermolecular vibrational modes – into which energy may be deposited without leading to autodetachment through destabilization of the loosely bound electron by large amplitude motions of the dipole configuration – than the dimer. This explanation can be further rationalized by the detailed balance relation (*e.g.* [51]) between the rate coefficient for electron attachment $k_e(E) = v\sigma_e(E)$, the autodetachment lifetime $\tau(E_-)$ and the densities of states of the neutral and the ionic clusters $\rho_0(E_0)$ and $\rho_-(E_-)$, respectively:

$$k_e(E)\tau(E_-) = \rho_-(E_-)/\rho_0(E_0), \qquad (4)$$

where $E_- = E + E_0 + AEA$. Since the density of states of the hexamer cluster anion is much larger than that for the dimer anion, the lifetime of the former is larger than that of the latter; hence the detection of hexamer anions is possible for larger electron energies. The gradual change in the overall shape of the energy dependence of the relative rate coefficients with increasing cluster size may be attributed to the evolution of a more strongly bound surface state, which influences the ion formation by electron attachment for $q \geq 7$.

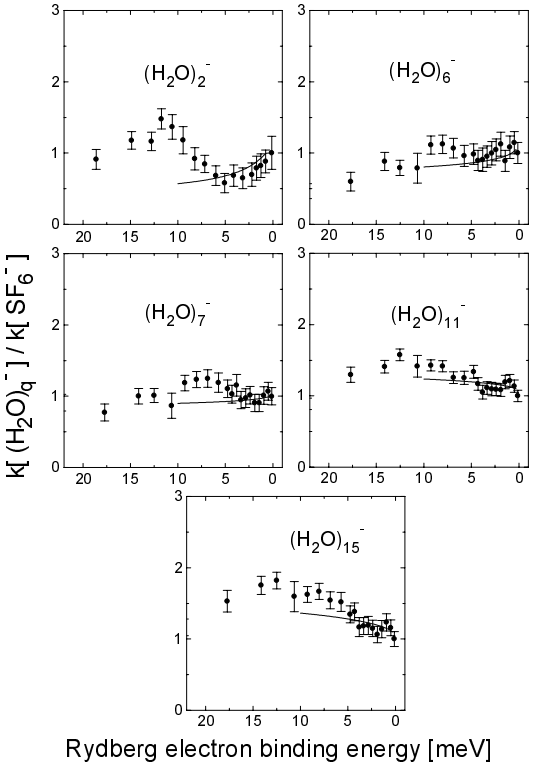

Fig. 4. Relative ratios of the rate coefficients for the formation of H_2O cluster ions and SF_6^- by Rydberg electron transfer (RET). The ratios have been derived by dividing the integrals over the respective mass peaks by that of the SF_6^- peak, and have been normalized to 1 for the highest principal quantum numbers ($n \approx 300$). The error bars represent the triple $\sqrt{N}$ errors of the peak integrals.

To compare free and Rydberg electrons, we have parameterized the energy dependence of the free electron ion formation cross-sections at very small electron energies by analytical functions (see Tab. 2) in order to calculate RET rate coefficients $k_{n\ell}$. As an analytical expression for the free electron cross-section for SF_6^- formation we used the expression (E in meV) [46,47]

$$\sigma_{e,SF_6}(E) \propto \frac{1}{E}\left[1 - \exp\left(-0.41\sqrt{E}\right)\right]. \qquad (5)$$

The respective resulting ratio of RET rate coefficients for the formation of $(H_2O)_q^-$ and SF_6^-, respectively, as calculated from equation (2) (using Rydberg electron velocity distributions for $\ell = 2$ from [21]) are shown in Figure 4 together with the measured relative RET rate coefficients. The calculated and the measured rate coefficients have been normalized to 1 at the highest principal quantum numbers ($n \approx 300$). One observes reasonable agreement from zero eV to Rydberg electron binding energies of $E_n \approx 5$ meV, corresponding to principal quantum numbers around $n = 52$. For higher Rydberg electron binding energies (lower n) the calculated results deviate substantially from the measured relative rate coefficients. We stress the fact that the analytical functions used in the calculations serve only as model

cross-sections for the energy range of 0–20 meV, *i.e.* the relevant energy range for RET in our calculations. We observe peaks in the RET rate coefficients (most clearly for the dimer anion at $E_n \approx 12$ meV, *i.e.* $n \approx 34$) at Rydberg binding energies in the range $E_n \approx 6$–15 meV ($n = 48$–30). According to the findings of Desfrancois and Schermann [23,24] for formation of dipole-bound anions of molecules and clusters in RET processes, a peak in the rate coefficient $k_{n\ell}$ located at a certain $n_{\max}$ can be correlated with a dipole-bound state (DBS) of binding energy $E_{\mathrm{DBS}} = 23 n_{\max}^{-2.9}$ eV, *i.e.* $E_{\mathrm{DBS}} \approx 1.7$–0.5 meV for $n_{\max} = 30$–48. Such weakly bound states may correspond to electrons attached to clusters with intermolecular vibrational excitation or to isomers with dipole moments just above the critical value. We note that we observe a second peak in the RET rate coefficient for dimer anion formation at $n = 13$ ($E_{\mathrm{DBS}} \approx 15$ meV), while for the other cluster sizes under study the RET rate coefficients continuously increase as n decreases down to $n = 12$ (not shown in Fig. 4), in qualitative accord with the results of Schermann and coworkers [17,35]. The formation of negative ions by resonant charge transfer into dipole bound states requires the assistance of the Rydberg core, showing that the free electron model is not valid in the case of such a process.

4 Conclusion

In summary, we have investigated the formation of small water cluster anions $(H_2O)_q^-$ in collisions with slow electrons at very high energy resolution. For the first time, we have observed "zero eV resonances" for the formation of water cluster ions with less than 10 molecules. Larger cluster ions are also formed at higher electron energies. We explain our results by assuming sufficiently rapid redistribution of the electronic excess energy into intermolecular vibrational modes, yielding metastable negative ions. Comparison of free and Rydberg electrons shows the validity limits of the free electron model due to the influence of the Rydberg core, but for sufficiently high principal quantum numbers a satisfactory agreement between calculated and measured relative RET rate coefficients is observed. More detailed theoretical work on the dynamics of metastable negative ion formation involving molecular clusters is desirable.

This work has been supported by the Deutsche Forschungsgemeinschaft (Schwerpunkt "Molekulare Cluster" and Forschergruppe "Niederenergetische Elektronenstreuprozesse"), by the Zentrum für Lasermeßtechnik und Diagnostik at the University of Kaiserslautern, and by the Graduiertenkolleg "Laser- und Teilchenspektroskopie".

References

1. J. Black, Philos. Trans. **65**, 124 (1775).
2. A.W. Castleman Jr, K.H. Bowen Jr, J. Phys. Chem. **100**, 12911 (1996).
3. J.V. Coe, A.D. Earhart, M.H. Cohen, G.J. Hoffman, H.W. Sarkas, K.H. Bowen, J. Chem. Phys. **107**, 6023 (1997).
4. S.S. Xantheas, T.H. Dunning Jr, J. Chem. Phys. **92**, 2806 (1990).
5. D.J. Wales, M.P. Hodges, Chem. Phys. Lett. **286**, 65 (1998).
6. J. Jortner, Z. Phys. D **24**, 247 (1992).
7. T.D. Märk, Int. J. Mass Spectrom. Ion Proc. **107**, 143 (1991).
8. E. Illenberger, Chem. Rev. **92**, 1589 (1992).
9. O. Ingólfsson, F. Weik, E. Illenberger, Int. J. Mass Spectrom. Ion Proc. **155**, 1 (1996).
10. T.D. Märk, K. Leiter, W. Ritter, A. Stamatovic, Phys. Rev. Lett. **55**, 2559 (1985).
11. M. Knapp, O. Echt, D. Kreisle, E. Recknagel, J. Chem. Phys. **85**, 636 (1986); Chem. Phys. Lett. **126**, 225 (1986); J. Phys. Chem. **91**, 2601 (1987).
12. M. Knapp, D. Kreisle, O. Echt, K. Sattler, E. Recknagel, Surf. Sci. **156**, 313 (1985).
13. S. Matejcik, A. Kiendler, P. Stampfli, A. Stamatovic, T.D. Märk, Phys. Rev. Lett. **77**, 3771 (1996).
14. J.M. Weber, E. Leber, M.-W. Ruf, H. Hotop, Phys. Rev. Lett. **82**, 516 (1999).
15. T. Kondow, J. Phys. Chem. **91**, 1307 (1987).
16. J. Kreil, M.-W. Ruf, H. Hotop, I. Ettischer, U. Buck, Chem. Phys. **239**, 459 (1998).
17. Y. Bouteiller, C. Desfrancois, H. Abdoul-Carime, J.P. Schermann, J. Chem. Phys. **105**, 6420 (1996).
18. P. Ayotte, M.A. Johnson, J. Chem. Phys. **106**, 811 (1997).
19. E. Fermi, Nuovo Cimento **11**, 157 (1934).
20. M. Matsuzawa, J. Chem. Phys. **55**, 2685 (1971); J. Phys. B **8**, 2114 (1975).
21. D. Klar, B. Mirbach, H.-J. Korsch, M.-W. Ruf, H. Hotop, Z. Phys. D **31**, 235 (1994).
22. F.B. Dunning, J. Phys. B **28**, 1645 (1995).
23. C. Desfrancois, Phys. Rev. A **51**, 3667 (1995).
24. C. Desfrancois, H. Abdoul-Carime, J.-P. Schermann, Int. J. Mod. Phys. B **12**, 1339 (1996).
25. R.N. Barnett, U. Landman, C.L. Cleveland, J. Jortner, J. Chem. Phys. **88**, 4429 (1988).
26. R.N. Barnett, U. Landman, S. Dhar, N.R. Kestner, J. Jortner, A. Nitzan, J. Chem. Phys. **91**, 7797 (1989).
27. P. Stampfli, Phys. Rep. **255**, 1 (1995).
28. S. Lee, S.J. Lee, J.Y. Lee, J. Kim, K.S. Kim, I. Park, K. Cho, J.D. Joanopoulos, Chem. Phys. Lett. **254**, 128 (1996).
29. K.S. Kim, I. Park, S. Lee, K. Cho, J.Y. Lee, J. Kim, J.D. Joannopoulos, Phys. Rev. Lett. **76**, 956 (1996).
30. S. Lee, J. Kim, S.J. Lee, K.S. Kim, Phys. Rev. Lett. **79**, 2038 (1997).
31. D.M.A. Smith, J. Smets, Y. Elkadi, L. Adamowicz, J. Chem. Phys. **109**, 1238 (1998).
32. T. Tsurusawa, S. Iwata, Chem. Phys. Lett. **287**, 553 (1998).
33. C. Desfrancois, H. Abdoul-Carime, N. Khelifa, J.P. Schermann, J. Chem. Phys. **102**, 4952 (1995).
34. H. Haberland, C. Ludewigt, H.-G. Schindler, D.R. Worsnop, J. Chem. Phys. **81**, 3742 (1984).
35. C. Desfrancois, A. Lisfi, J.P. Schermann, Z. Phys. D **24**, 297 (1992).
36. C. Desfrancois, B. Baillon, J.P. Schermann, S.T. Arnold, J.H. Hendricks, K.H. Bowen, Phys. Rev. Lett. **72**, 48 (1994).

37. H. Abdoul-Carime, A. Wakisaka, Y. Bouteiller, C. Desfrancois, J.P. Schermann, Z. Phys. D **40**, 55 (1997).
38. L.A. Posey, P. Campagnola, M.A. Johnson, G.H. Lee, G.H. Eaton, K.H. Bowen, J. Chem. Phys. **91**, 6536 (1989).
39. J.V. Coe, G.H. Lee, J.G. Eaton, S.T. Arnold, H.W. Sarkas, K.H. Bowen, C. Ludewigt, H. Haberland, D.R. Worsnop, J. Chem. Phys. **92**, 3980 (1990).
40. P.J. Campagnola, D.J. Lavrich, M.J. DeLuca, M.A. Johnson, J. Chem. Phys. **94**, 5240 (1991).
41. C.G. Bailey, J. Kim, M.A. Johnson, J. Phys. Chem. **100**, 16782 (1996).
42. C.G. Bailey, M.A. Johnson, Chem. Phys. Lett. **265**, 185 (1997).
43. J. Kim, C. Bailey, I. Becker, O. Cheshnovsky, M.A. Johnson, Chem. Phys. Lett. **297**, 90 (1998).
44. P.J. Campagnola, D.M. Cyr, M.A. Johnson, Chem. Phys. Lett. **181**, 206 (1991).
45. S.T. Arnold, R.A. Morris, A.A. Viggiano, J. Chem. Phys. **103**, 9242 (1995).
46. D. Klar, M.-W. Ruf, H. Hotop, Chem. Phys. Lett. **45**, 263 (1992).
47. D. Klar, M.-W. Ruf, H. Hotop, Meas. Sci. Technol. **5**, 1248 (1994).
48. H. Hotop, D. Klar, J. Kreil, M.-W. Ruf, A. Schramm, J.M. Weber, in *The Physics of Electronic and Atomic Collisions*, edited by L.J. Dubé, J.B.A. Mitchell, J.W. McConkey, C.E. Brion, XIX Int. Conference, Whistler, Canada, July-August 1995, AIP Conference Proceedings 360 (AIP Press, American Institute of Physics, Woodbury, New York, 1995), pp. 267-78
49. A. Schramm, J.M. Weber, J. Kreil, D. Klar, M.-W. Ruf, H. Hotop, Phys. Rev. Lett. **81**, 778 (1998).
50. R. Knochenmuss, S. Leutwyler, J. Chem. Phys. **96**, 5233 (1996).
51. R.N. Compton, in *Photophysics and Photochemistry in the Vacuum Ultraviolet*, edited by S.P. McGlynn *et al.* (D. Reidel Publ. Co., 1985), p. 261.
52. C.E. Klots, Chem. Phys. Lett. **186**, 61 (1976).